

Spatio-Temporal Models to Support Small Area Estimation: Applications to National-Scale Forest Carbon Monitoring

Elliot S. Shannon^{1,2} and Andrew O. Finley^{1,2}

¹Dept. of Forestry, Michigan State University, East Lansing, MI, USA.

²Dept. of Statistics and Probability, Michigan State University, East Lansing, MI, USA.

April 4, 2025

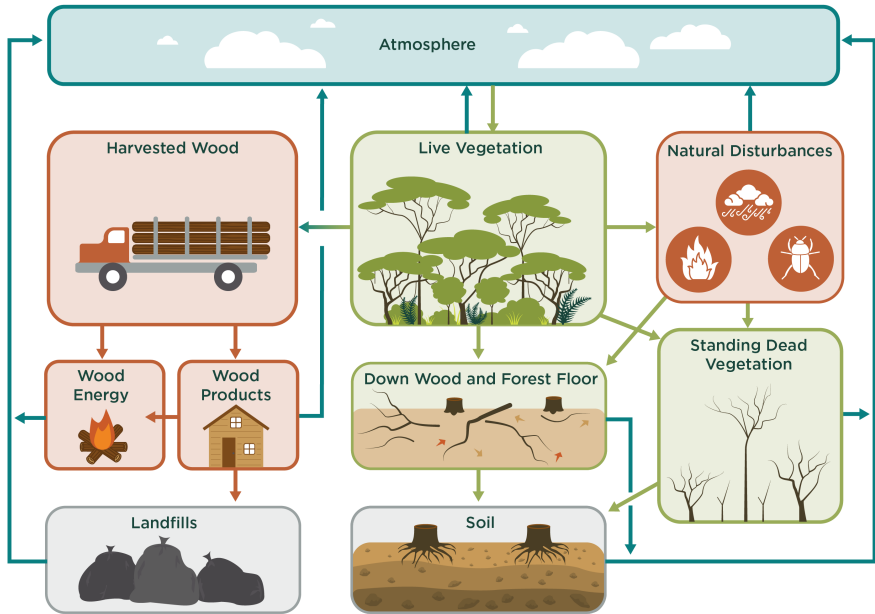
Motivation

The United Nations Framework Convention on Climate Change (UNFCCC) requires annual greenhouse gas (GHG) emission estimates (with uncertainty quantification) from five sectors:

- Energy
- Industry
- Agriculture
- **Forestry**
- Waste



Carbon Cycle



National Forest Inventory and FIA

- Forest carbon estimates are based on National Forest Inventory (NFI) data and estimators.
- The US NFI is conducted by the USDA Forest Service Forest Inventory and Analysis (FIA) program.
- FIA maintains 300,000 inventory plots across the contiguous US (CONUS), which are measured on rotating basis every 5 to 10 years.

FIA Design

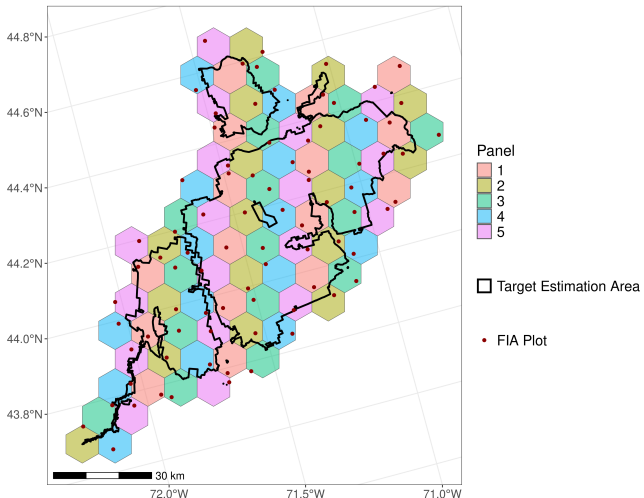


Figure 1: FIA sampling design (May and Finley, 2025).

Design-based Estimation

- Traditionally, NFI programs provide design-based estimates for forest parameters based on forest inventory plot measurements.
- Design-based estimates assume a fixed finite population, with population parameters accessible without error if all population units are observed.
- To achieve desired levels of estimate precision, these methods require repeated costly measurements from a dense network of inventory plots.
- Given the high costs associated with data acquisition, FIA plot measurements are sparse, limiting reliable design-based estimates to large spatial and temporal scales.

Demand for Small Area Estimates

Increasingly, users groups require higher spatial and temporal resolution forest status and change parameter estimates to evaluate existing land use policies and management practices, and inform future activities.



FIA has made it a priority to deliver statistically rigorous annual county-level estimates of forest parameters to support user needs.

Small Area Estimation

- Model-based small area estimation (SAE) methods have gained attention for estimating forest parameters in data-sparse settings (Schroeder et al., 2014; Lister et al., 2020; Hou et al., 2021; Coulston et al., 2021; Finley et al., 2024; Shannon et al., 2024)
- SAE methods employ statistical models to relate forest response variables to auxiliary data.
- Accuracy and precision are improved over design-based approaches when strong relationships exist between response variables and auxiliary information.

Inferential Objectives, Models, and Data

We seek SAE models to estimate the parameters of interest at desired spatial and/or temporal resolutions, e.g., status at a given time or change over time for user-defined small areas.

- Model formulation depends on the inferential objectives and the assumed data generating process.
- From a practical standpoint, model formulation also depends data availability.

We formulate models presumed to capture the underlying data generating process and tailored to match available data.

We are curious about how quality of inference changes given varying degrees of information.

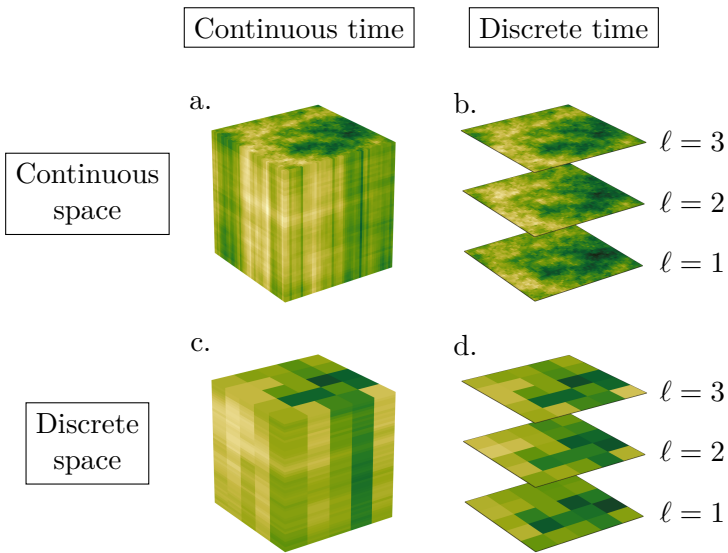


Figure 2: Data generation settings.

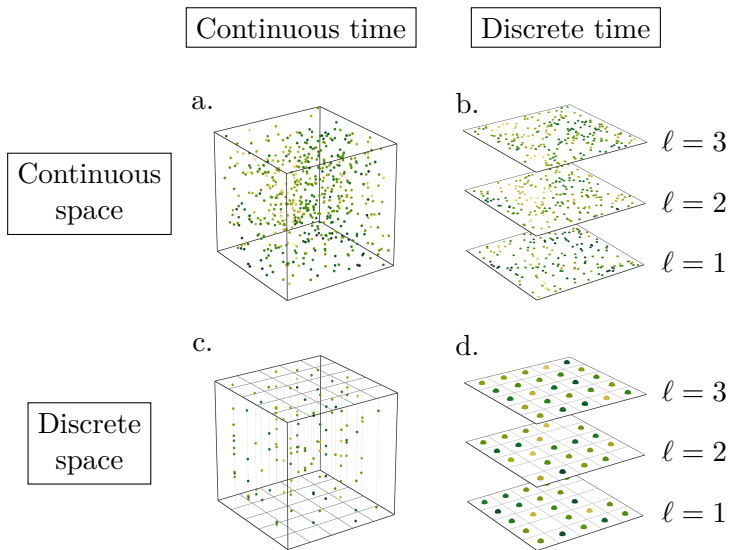
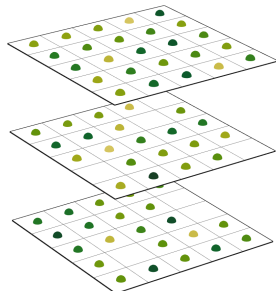
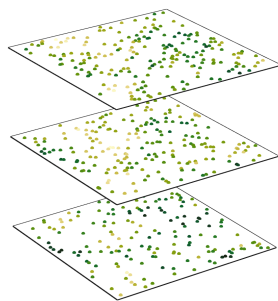


Figure 3: Data observation settings corresponding to Figure 2.

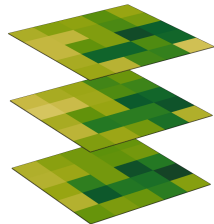
Unit-level vs. Area-level SAE methods

- **Unit-level** models are constructed at the population unit level (inventory plots), which is the minimal unit that can be sampled from a population.
- **Area-level** models characterize the relationship between area-specific (design-based) direct estimates and auxiliary data.



Motivating Data and Estimates

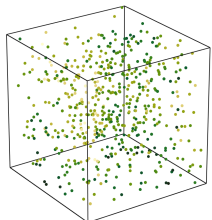
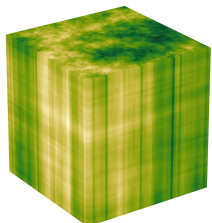
- Investigate spatio-temporal SAE models for forest parameters of interest under different data/model settings (Figures 2 and 3).
- We focus on live above ground carbon (carbon) (Mg/ha), which is estimated as part of the FIA NFI.
- Our latent parameter of interest is annual mean carbon (Mg/ha) for each county in the CONUS from 2008-2021.



Continuous Space-time Unit-level Model Notation

Assume unit-level mean carbon measurements are generated from a continuous spatio-temporal process. Let

- $y(\mathbf{s}, t)$ be the mean carbon (Mg/ha) at spatial coordinate \mathbf{s} and time t .
- $\mathbf{x}(\mathbf{s}, t)$ be a length $P + 1$ vector of covariates associated with $y(\mathbf{s}, t)$, where the first element of $\mathbf{x}(\mathbf{s}, t)$ is 1.
- $\mu_{j,\ell}$ be the mean carbon for county j and year ℓ , where $j = 1, \dots, \mathcal{J}$ and $\ell = 1, \dots, \mathcal{L}$.
- \mathcal{A}_j be the spatial area constituting county j .



Continuous Space-time Unit-level Model

The proposed continuous space-time unit-level spatio-temporal SAE model is

$$\begin{aligned} y(\mathbf{s}, t) &= \mu(\mathbf{s}, t) + \delta(\mathbf{s}, t), \\ \mu(\mathbf{s}, t) &= \mathbf{x}(\mathbf{s}, t)^T \boldsymbol{\beta}(t) + u(\mathbf{s}, t) + \varepsilon(\mathbf{s}, t) \\ \boldsymbol{\beta}_p(t) &\sim \text{GP}_{\text{T}}(m_{\beta_p}, C_{\beta}(\cdot, \boldsymbol{\theta}_{\beta_p})), \quad p = 1, \dots, P+1, \\ u(\mathbf{s}, t) &\sim \text{GP}_{\text{ST}}(\mathbf{0}, C_u(\cdot, \boldsymbol{\theta}_u)), \end{aligned} \tag{1}$$

where

- $\delta(\mathbf{s}, t) \stackrel{\text{iid}}{\sim} N(0, \sigma_j^2)$ for $\mathbf{s} \in \mathcal{A}_j$.
- $\varepsilon(\mathbf{s}, t) \stackrel{\text{iid}}{\sim} N(0, \tau_{\ell}^2)$ for $\ell - 0.5 < t < \ell + 0.5$.
- $\boldsymbol{\beta}(t) = (\beta_1(t), \dots, \beta_{P+1}(t))^T$ is a vector of regression coefficients whose p^{th} element follows a temporal GP.
- $u(\mathbf{s}, t)$ is a random intercept following a spatio-temporal GP with covariance function $C_u(\cdot, \boldsymbol{\theta}_u)$.

Modeling Covariates

Often, covariates $\mathbf{x}(s, t)$ are not available for all s and t , so we can extend (1) as

$$\begin{aligned}y(s, t) &= \mu(s, t) + \delta(s, t), \\ \mu(s, t) &= \mathbf{x}(s, t)^T \boldsymbol{\beta}(t) + u(s, t) + \varepsilon(s, t) \\ \mathbf{x}(s, t) &\sim \text{GP}_{\text{ST}}(m_{\mathbf{x}}, C_{\mathbf{x}}(\cdot, \boldsymbol{\theta}_{\mathbf{x}})), \\ \boldsymbol{\beta}_p(t) &\sim \text{GP}_{\text{T}}(m_{\beta_p}, C_{\beta}(\cdot, \boldsymbol{\theta}_{\beta_p})), \quad p = 1, \dots, P + 1, \\ u(s, t) &\sim \text{GP}_{\text{ST}}(\mathbf{0}, C_u(\cdot, \boldsymbol{\theta}_u)),\end{aligned}\tag{2}$$

where

- $\text{GP}_{\text{ST}}(m_{\mathbf{x}}, C_{\mathbf{x}}(\cdot, \boldsymbol{\theta}_{\mathbf{x}}))$ is a spatio-temporal GP with mean function $m_{\mathbf{x}}$ and covariance function $C_{\mathbf{x}}(\cdot, \boldsymbol{\theta}_{\mathbf{x}})$ taking parameters $\boldsymbol{\theta}_{\mathbf{x}}$.

Spatio-temporal Random Intercept

We model $u(\mathbf{s}, t) \sim \text{GP}_{\text{ST}}(\mathbf{0}, C_u(\cdot, \boldsymbol{\theta}_u))$ as a mean-zero spatio-temporal GP with covariance function $C_u(\cdot, \boldsymbol{\theta}_u)$.

For locations \mathbf{s}_1 and \mathbf{s}_2 and times t_1 and t_2 , the covariance between $u(\mathbf{s}_1, t_1)$ and $u(\mathbf{s}_2, t_2)$ might be modeled using a nonseparable covariance function, e.g.,

$$\frac{\sigma_u^2}{(a_u|r|^2 + 1)^{\kappa_u}} \exp\left(\frac{-c_u\|h\|}{(a_u|r|^2 + 1)^{\kappa_u/2}}\right) \quad (3)$$

where $r = |t_1 - t_2|$ and $h = \|\mathbf{s}_1 - \mathbf{s}_2\|$ are the time and space euclidean norms, respectively, and $\boldsymbol{\theta}_u = (\sigma_u^2, a_u, c_u, \kappa_u)$. See Datta et al. (2016) for details.

A better option is a multi-resolution space-time covariance function recently explored by May and Finley (2025).

Estimating $\mu_{j,\ell}$

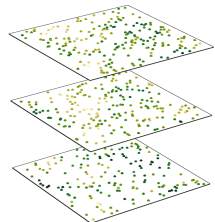
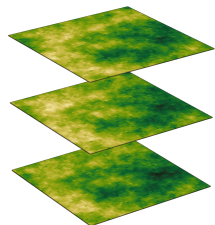
- Estimates of $\mu_{j,\ell}$ from fitted models (1) or (2) are obtained via block kriging.
- For county j in year ℓ , the fitted model is used to predict $\mu(\mathbf{s}, t)$ for a dense grid of points $\mathcal{P}_{j,\ell}$, where each prediction point has $\mathbf{s} \in \mathcal{A}_j$ and $\ell - 0.5 < t < \ell + 0.5$.
- The block kriging estimate for $\mu_{j,\ell}$ is then

$$\hat{\mu}_{j,\ell} = \frac{1}{|\mathcal{P}_{j,\ell}|} \sum_{(\mathbf{s},t) \in \mathcal{P}_{j,\ell}} \mu(\mathbf{s}, t). \quad (4)$$

Dynamic Unit-level Model Notation

Assume unit-level mean carbon measurements are generated from a continuous spatial process, which evolves dynamically over discrete time. Let

- $y_\ell(\mathbf{s})$ be the mean carbon (Mg/ha) at spatial coordinate \mathbf{s} in year ℓ .
- $\mathbf{x}_\ell(\mathbf{s})$ be a length $P + 1$ vector of covariates associated with $y_\ell(\mathbf{s})$, where the first element of $\mathbf{x}_\ell(\mathbf{s})$ is 1.



Dynamic Unit-level Model

The proposed dynamic unit-level spatio-temporal SAE model is then

$$\begin{aligned}y_\ell(\mathbf{s}) &= \mu_\ell(\mathbf{s}) + \delta_\ell(\mathbf{s}), \\ \mu_\ell(\mathbf{s}) &= \mathbf{x}_\ell(\mathbf{s})^T \boldsymbol{\beta}_\ell + u_\ell(\mathbf{s}) + \varepsilon_\ell(\mathbf{s}), \\ \boldsymbol{\beta}_\ell &= \boldsymbol{\beta}_{\ell-1} + \boldsymbol{\xi}_\ell, \quad \boldsymbol{\xi}_\ell \sim MVN(\mathbf{0}, \boldsymbol{\Sigma}_\xi), \\ u_\ell(\mathbf{s}) &= u_{\ell-1}(\mathbf{s}) + \omega_\ell(\mathbf{s}), \quad \omega_\ell \sim GP_S(\mathbf{0}, C_\omega(\cdot, \boldsymbol{\theta}_\ell)), \\ u_0(\mathbf{s}) &\equiv 0 \quad \forall \mathbf{s}\end{aligned}\tag{5}$$

where

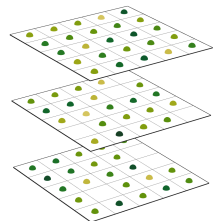
- $\delta_\ell(\mathbf{s}) \stackrel{\text{iid}}{\sim} N(0, \sigma_j^2)$ for $\mathbf{s} \in \mathcal{A}_j$.
- $\varepsilon_\ell(\mathbf{s}) \stackrel{\text{iid}}{\sim} N(0, \tau_\ell^2)$.
- $\boldsymbol{\beta}_0 \sim MVN(\boldsymbol{\mu}_0, \boldsymbol{\Sigma}_0)$.

Estimates of $\mu_{j,\ell}$ are obtained via (4).

Plot-aggregate Dynamic Models

To protect private forest land information and preserve the ecological integrity of the plots, exact plot locations are not publicly available for most NFIs. Two cases are common:

- ① Unit-level measurements can often still be associated with areas of interest, and may be modeled directly (Shannon et al., 2025),
- ② Traditionally, SAE methods such as the Fay-Herriot model (Fay and Herriot, 1979) model aggregated direct estimates for small areas of interest (Shannon et al., 2024).

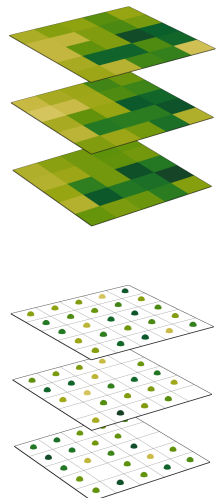


Dynamic Unit-level Plot-aggregate Model Notation

Assume unit-level mean carbon measurements are generated from a discrete spatial random field, which evolves dynamically over time. Exact plot locations are not known, but measurements are associated with discrete areas. Let

- $y_{i,j,\ell}$ be the mean carbon (Mg/ha) at for inventory plot i in county j in year ℓ , where $i = 1, \dots, n_{j,\ell}$.
- $\mathbf{x}_{j,\ell}$ be a length $P + 1$ vector of covariates associated with county j in year ℓ , where the first element of $\mathbf{x}_{j,\ell}$ is 1.

Note, we may have $n_{j,\ell} = 0$.



Dynamic Unit-level Plot-aggregate Model

The model proposed by Shannon et al. (2025) is

$$\begin{aligned}y_{i,j,\ell} &= \underbrace{\mathbf{x}_{j,\ell}^T \boldsymbol{\beta}_\ell + \tilde{\mathbf{x}}_{j,\ell}^T \boldsymbol{\eta}_j + u_{j,\ell}}_{\mu_{j,t}} + \varepsilon_{i,j,\ell}, \quad i = 1, \dots, n_{j,t}, \\ \boldsymbol{\beta}_\ell &= \boldsymbol{\beta}_{\ell-1} + \boldsymbol{\xi}_\ell, \quad \boldsymbol{\xi}_\ell \sim MVN(\mathbf{0}, \boldsymbol{\Sigma}_\xi), \\ u_{j,\ell} &= u_{j,\ell-1} + \omega_{j,\ell}, \quad \boldsymbol{\omega}_\ell \sim MVN\left(\mathbf{0}, \tau_{\omega,t}^2 \mathbf{Q}(\rho_\omega)\right), \\ u_{j,0} &\equiv 0 \quad \forall j = 1, \dots, \mathcal{J},\end{aligned}\tag{6}$$

where

- $\varepsilon_{i,j,\ell} \stackrel{\text{ind}}{\sim} N(0, \tau_\ell^2)$.
- $\tilde{\mathbf{x}}_{j,\ell}$ is a length $Q \leq P$ subvector of covariates in $\mathbf{x}_{j,\ell}$.
- $\boldsymbol{\eta}_j$ is a length Q vector of county-varying regression coefficients.
- $\boldsymbol{\beta}_0 \sim MVN(\boldsymbol{\mu}_0, \boldsymbol{\Sigma}_0)$.

County-varying Regression Coefficients $\boldsymbol{\eta}_j$

- The elements of $\boldsymbol{\eta}_j$ in (6) represent county-varying regression coefficients for covariates in $\tilde{\mathbf{x}}_{j,\ell}$, which follow a conditional autoregressive (CAR) model structure (Banerjee et al., 2004).
- Writing $\boldsymbol{\eta}_j = (\eta_{1,j}, \dots, \eta_{Q,j})^T$ and collecting $\boldsymbol{\eta}_q^* = (\eta_{q,1}, \dots, \eta_{q,J})^T$, the CAR spatial structure for $\boldsymbol{\eta}_q^*$ is specified as

$$\boldsymbol{\eta}_q^* \sim MVN \left(\mathbf{0}, \tau_{\eta,q}^2 \mathbf{Q}(\rho_{\eta,q}) \right), \quad q = 1, \dots, Q, \quad (7)$$

where

- $\tau_{\eta,q}^2$ is a scalar variance parameter.
- $\rho_{\eta,q}$ is a spatial correlation parameter ($0 < \rho_{\eta,q} < 1$).
- $\mathbf{Q}(\rho_{\eta,q}) = (\mathbf{D} - \rho_{\eta,q} \mathbf{W})^{-1}$ is a $J \times J$ correlation matrix.
- \mathbf{W} is a binary spatial adjacency matrix with $w_{j,j} = 0$ for all j .
- $\mathbf{D} = \text{diag}(\text{rowSums}(\mathbf{W}))$.

Dynamic spatio-temporal intercept $u_{j,\ell}$

- The spatio-temporally varying intercept term $u_{j,\ell}$ in (6) is modeled as a dynamically evolving CAR spatial random effect.

$$u_{j,\ell} = u_{j,\ell-1} + \omega_{j,\ell}, \quad (8)$$

- We model $\mathbf{u}_\ell = (u_{1,\ell}, \dots, u_{J,\ell})^\top$ as a dynamically evolving CAR spatial random effect.
- Collecting all $\omega_{j,\ell}$ for year ℓ as $\boldsymbol{\omega}_\ell = (\omega_{1,\ell}, \dots, \omega_{J,\ell})^\top$, we specify a CAR spatial structure for $\boldsymbol{\omega}_\ell$ as

$$\boldsymbol{\omega}_\ell \sim MVN \left(\mathbf{0}, \tau_{\omega,\ell}^2 \mathbf{Q}(\rho_\omega) \right). \quad (9)$$

Alternatively, continuous spatial structures such as GPs could be used to model $\boldsymbol{\omega}_\ell$ over county centroids.

Priors and Likelihood

The joint posterior distribution for all parameters in model (6) is then proportional to the product of the likelihood times priors, which is given as

$$\begin{aligned} & \prod_{\ell=1}^{\mathcal{L}} \prod_{j=1}^{\mathcal{J}} \prod_{i=1}^{n_{j,\ell}} N \left(y_{i,j,\ell} \mid \mathbf{x}_{j,\ell}^T \boldsymbol{\beta}_\ell + \tilde{\mathbf{x}}_{j,\ell}^T \boldsymbol{\eta}_j + u_{j,\ell}, \sigma_\ell^2 \right) \times \prod_{\ell=1}^{\mathcal{L}} IG \left(\sigma_\ell^2 \mid a_\sigma, b_\sigma \right) \times \\ & MVN \left(\boldsymbol{\beta}_0 \mid \boldsymbol{\mu}_0, \boldsymbol{\Sigma}_0 \right) \times \prod_{\ell=1}^{\mathcal{L}} MVN \left(\boldsymbol{\beta}_\ell \mid \boldsymbol{\beta}_{\ell-1}, \boldsymbol{\Sigma}_\xi \right) \times IW \left(\boldsymbol{\Sigma}_\xi \mid \nu_\xi, \mathbf{H}_\xi \right) \times \\ & \prod_{q=1}^Q MVN \left(\boldsymbol{\eta}_q^* \mid \mathbf{0}, \tau_{\eta,q}^2 \mathbf{Q}(\rho_{\eta,q}) \right) \times \prod_{q=1}^Q IG \left(\tau_{\eta,q}^2 \mid a_{\eta,q}, b_{\eta,q} \right) \times \prod_{q=1}^Q U \left(\rho_{\eta,q} \mid 0, 1 \right) \times \\ & \prod_{\ell=1}^{\mathcal{L}} MVN \left(\mathbf{u}_\ell \mid \mathbf{u}_{\ell-1}, \tau_{\omega,\ell}^2 \mathbf{Q}(\rho_\omega) \right) \times \prod_{\ell=1}^{\mathcal{L}} IG \left(\tau_{\omega,\ell}^2 \mid a_{\omega,\ell}, b_{\omega,\ell} \right) \times U \left(\rho_\omega \mid 0, 1 \right). \end{aligned} \tag{10}$$

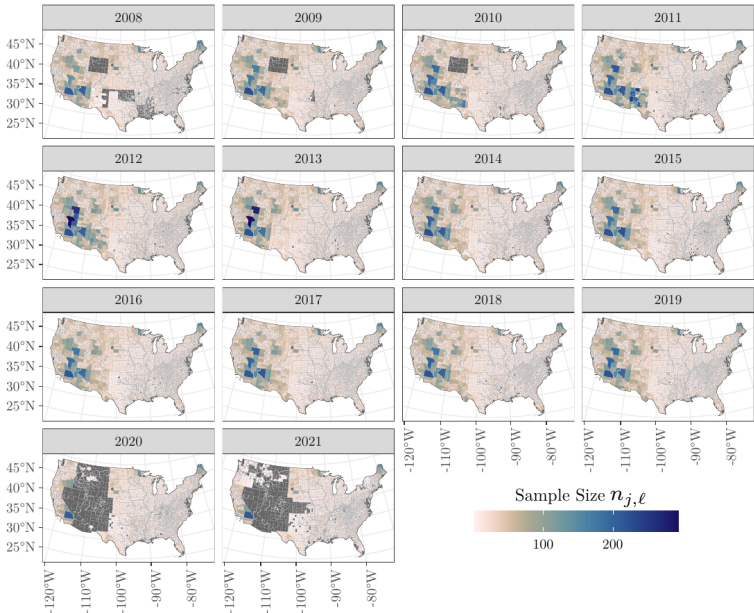
Methods

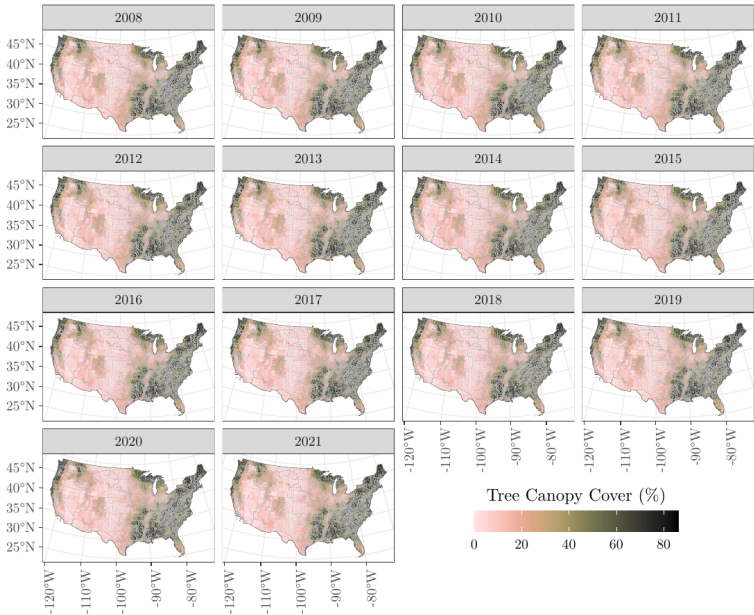
- Model (6) was fit by Shannon et al. (2025) using 593,368 FIA plot measurements from 2008-2021 across the CONUS.
- Percent tree canopy cover (TCC) was used as a single covariate ($P = Q = 1$).
- M MCMC samples of $\mu_{j,\ell}$ were used to estimate linear trends over time, whose posterior inference is available via

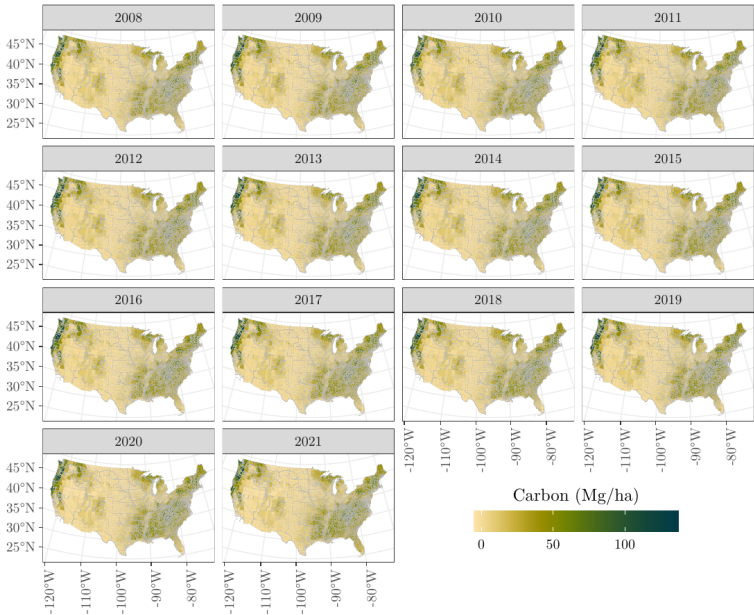
$$\theta_j^m = \frac{\sum_{\ell=1}^L (\ell - \bar{\ell}) (\mu_{j,\ell}^m - \bar{\mu}_j^m)}{\sum_{\ell=1}^L (\ell - \bar{\ell})^2}, \quad m = 1, \dots, M, \quad (11)$$

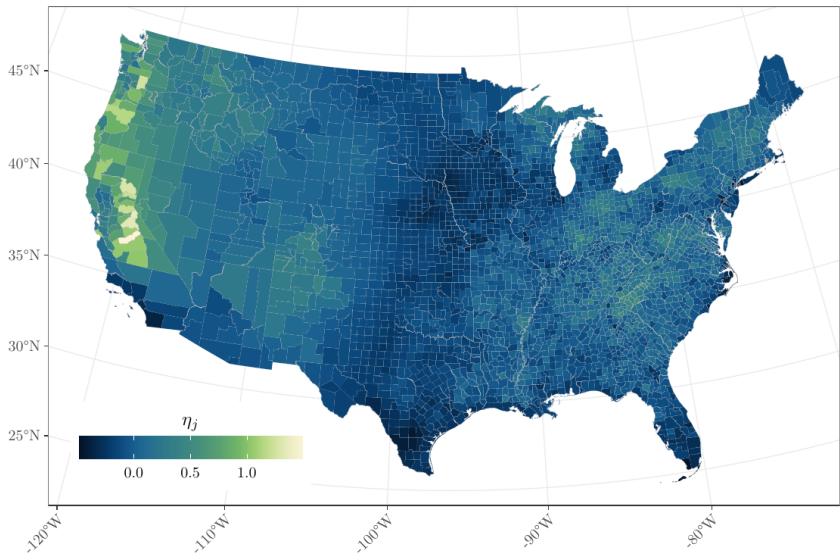
where

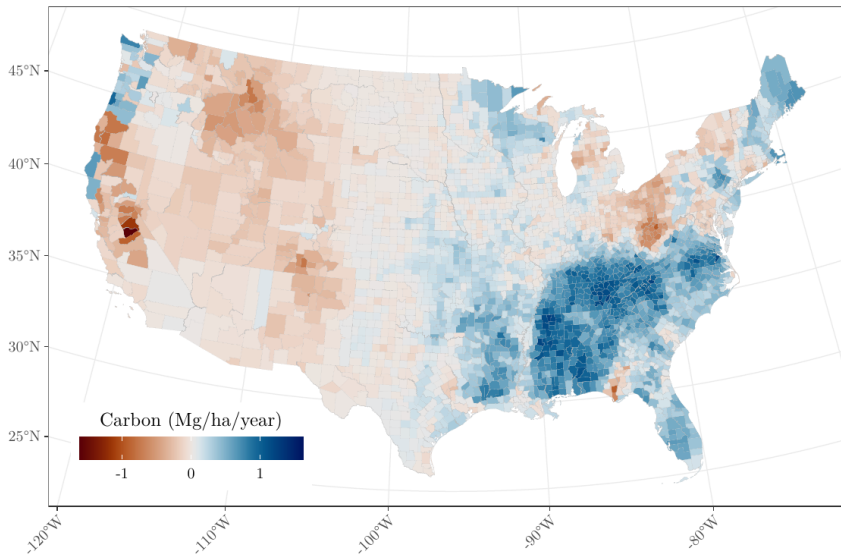
- $\bar{\ell} = \frac{1}{L} \sum_{\ell=1}^L \ell$.
- $\bar{\mu}_j^m = \frac{1}{L} \sum_{\ell=1}^L \mu_{j,\ell}^m$.
- Trend significance is determined by observing if the 95% credible interval for θ_j overlaps zero.

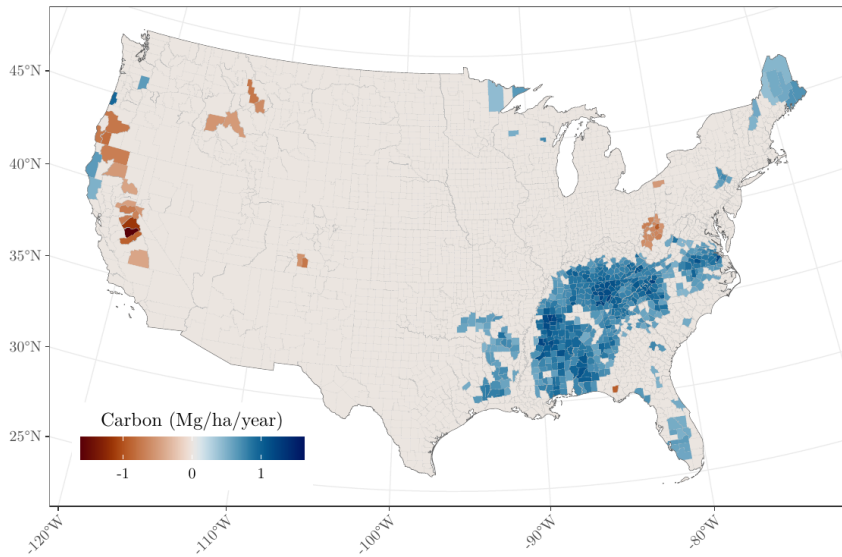




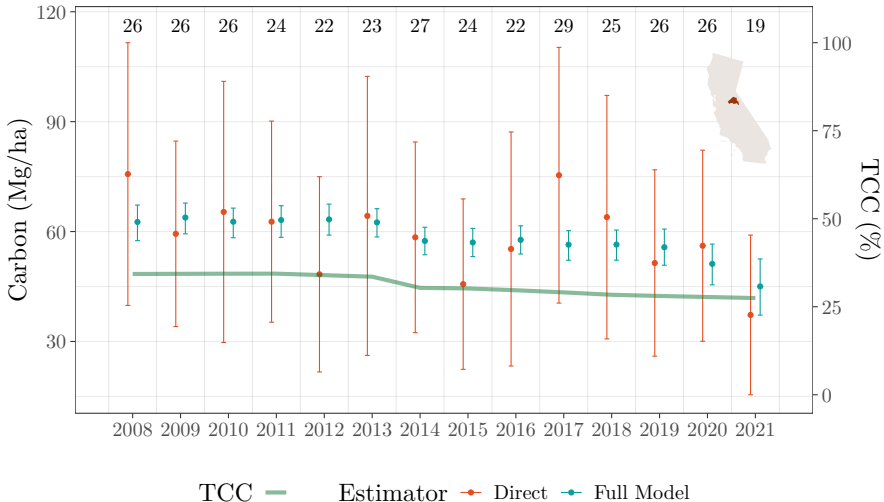








Tuolumne, California



In 2013 the Rim Fire burned 257,314 acres and is clearly seen in the SAE model estimates.

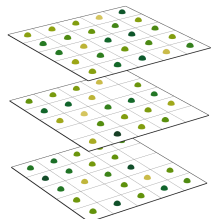
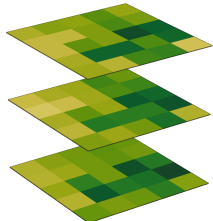
Direct Estimates

- Assume individual plot-level measurements are unavailable, and instead we only have direct estimates for small areas of interest.
- The direct estimate mean for county j in year ℓ is

$$\hat{\mu}_{j,\ell} = \frac{1}{n_{j,\ell}} \sum_{i=1}^{n_{j,\ell}} y_{i,j,\ell}. \quad (12)$$

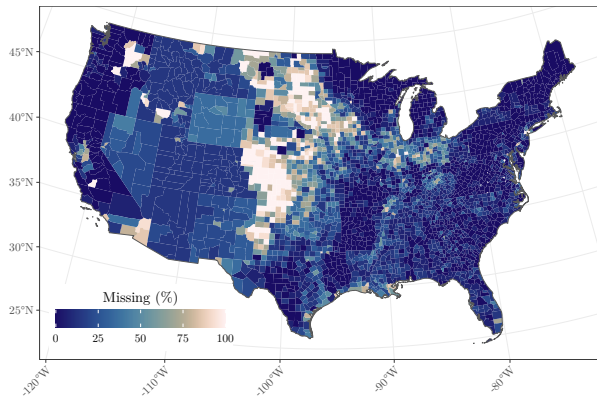
- The associated estimate variance is

$$\hat{\sigma}_{j,\ell}^2 = \frac{1}{n_{j,\ell}(n_{j,\ell} - 1)} \sum_{i=1}^{n_{j,\ell}} (y_{i,j,\ell} - \hat{\mu}_{j,\ell})^2. \quad (13)$$



Missing Direct Estimates

- When $n_{j,\ell} \in \{0, 1\}$, direct estimates (12) and/or (13) will be missing.
- Direct estimate (13) is also missing when plot measurements in county j at year ℓ are identical.
- In these cases, we still aim to produce an estimate for $\mu_{j,\ell}$.



Dynamic Area-level Plot-aggregate Model

The model proposed by Shannon et al. (2024) is

$$\begin{aligned}\hat{\mu}_{j,\ell} &= \mu_{j,\ell} + \delta_{j,\ell}, \\ \mu_{j,\ell} &= \mathbf{x}_{j,\ell}^T \boldsymbol{\beta} + \tilde{\mathbf{x}}_{j,\ell}^T \boldsymbol{\eta}_j + u_{j,\ell} + \varepsilon_{j,\ell}, \\ \mathbf{u} &\sim MVN \left(\mathbf{0}, \sigma_u^2 \mathbf{R}(\rho_u) \otimes \mathbf{A}(\alpha_u) \right),\end{aligned}\tag{14}$$

where

- $\delta_{j,\ell} \stackrel{\text{ind}}{\sim} N(0, \sigma_{\delta,j,\ell}^2)$ and $\epsilon_{j,\ell} \stackrel{\text{iid}}{\sim} N(0, \sigma_\epsilon^2)$.
- $\mathbf{u} = (\mathbf{u}_1^T, \dots, \mathbf{u}_L^T)^T$ is the length $\mathcal{J} \times \mathcal{L}$ vector of spatio-temporal random effects.
- $\mathbf{R}(\rho_u) = (\mathbf{D} - \rho_u \mathbf{W})^{-1}$ is the $\mathcal{J} \times \mathcal{J}$ CAR correlation matrix.
- $\mathbf{A}(\alpha_u)$ is a $\mathcal{L} \times \mathcal{L}$ first order autoregressive correlation matrix with temporal correlation parameter α_u and ij^{th} element equal to $\alpha_u^{|i-j|}$.

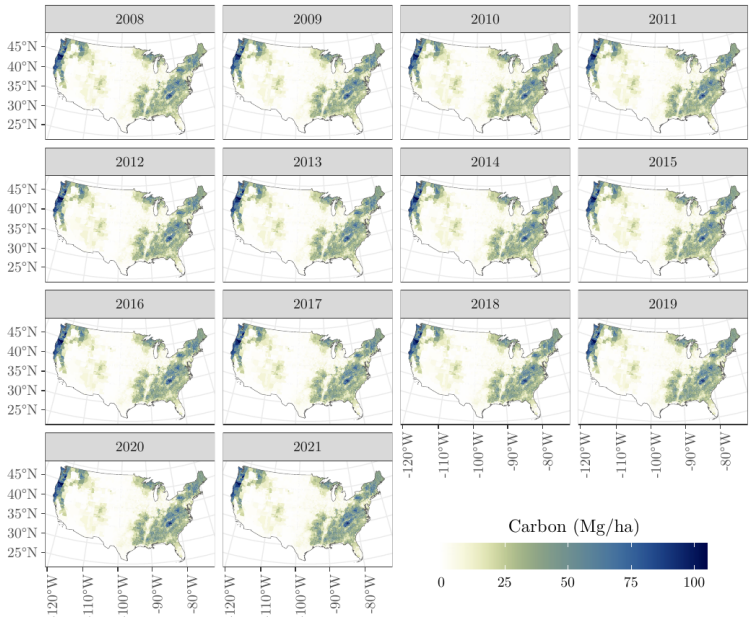
Priors and Likelihood

The joint posterior distribution for all parameters in model (14) is then proportional to the product of the likelihood times priors, which is given as

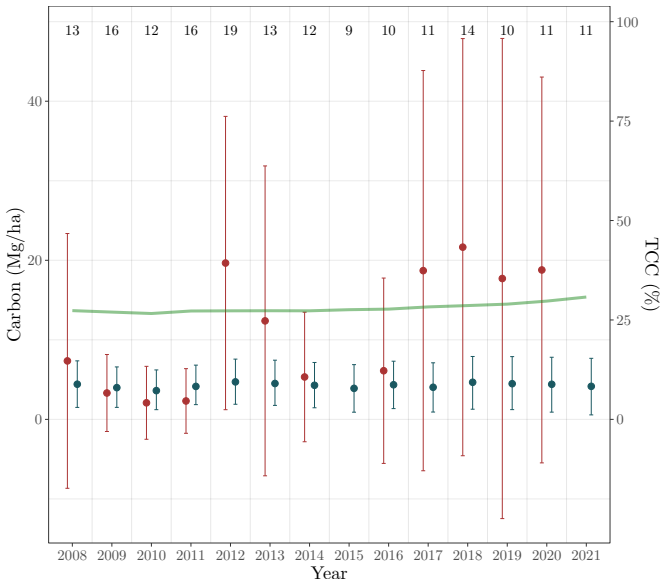
$$\begin{aligned} & \prod_{j=1}^J \prod_{\ell=1}^{\mathcal{L}} N\left(\hat{\mu}_{j,\ell} \mid \mu_{j,\ell}, \sigma_{j,\ell}^2\right) \times \prod_{j=1}^J \prod_{\ell=1}^{\mathcal{L}} N\left(\mu_{j,\ell} \mid \mathbf{x}_{j,\ell}^T \boldsymbol{\beta} + \tilde{\mathbf{x}}_{j,\ell}^T \boldsymbol{\eta}_j + u_{j,\ell}, \sigma_{\epsilon}^2\right) \times \\ & MVN(\boldsymbol{\beta} \mid \boldsymbol{\mu}_{\beta}, \boldsymbol{\Sigma}_{\beta}) \times \prod_{j=1}^J \prod_{\ell=1}^{\mathcal{L}} IG\left(\sigma_{j,\ell}^2 \mid \frac{n_{j,\ell}}{2}, \frac{(n_{j,\ell}-1) \hat{\sigma}_{j,\ell}^2}{2}\right) \times \\ & IG\left(\sigma_{\epsilon}^2 \mid a_{\epsilon}, b_{\epsilon}\right) \times MVN\left(\mathbf{u} \mid \mathbf{0}, \sigma_u^2 \mathbf{R}(\rho_u) \otimes \mathbf{A}(\alpha_u)\right) \times \\ & IG\left(\sigma_u^2 \mid a_u, b_u\right) \times U(\rho_u \mid a_{\rho}, b_{\rho}) \times U(\alpha_u \mid a_{\alpha}, b_{\alpha}) \times \\ & \prod_{q=1}^Q MVN\left(\boldsymbol{\eta}_q^* \mid \mathbf{0}, \sigma_{\eta,q}^2 \mathbf{R}(\rho_{\eta,q})\right) \times \prod_{q=1}^Q IG\left(\sigma_{\eta,q}^2 \mid a_{\eta,q}, b_{\eta,q}\right) \times \prod_{q=1}^Q U(\rho_{\eta,q} \mid 0, 1). \end{aligned}$$

Results

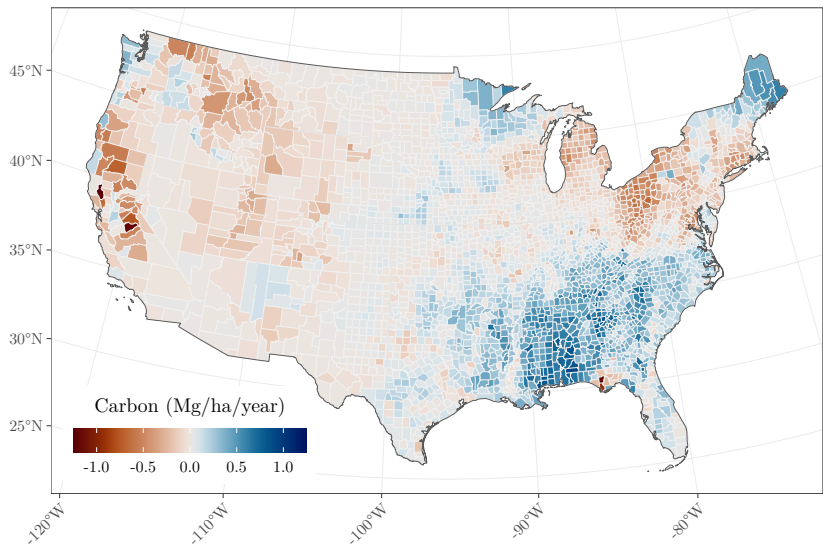
- Model (14) was fit by Shannon et al. (2024) using 32,885 annual county-level direct estimates from 2008-2021 across the CONUS.
- Percent tree canopy cover (TCC) was used as a single covariate ($P = Q = 1$).
- Linear trends were estimated as in (11).

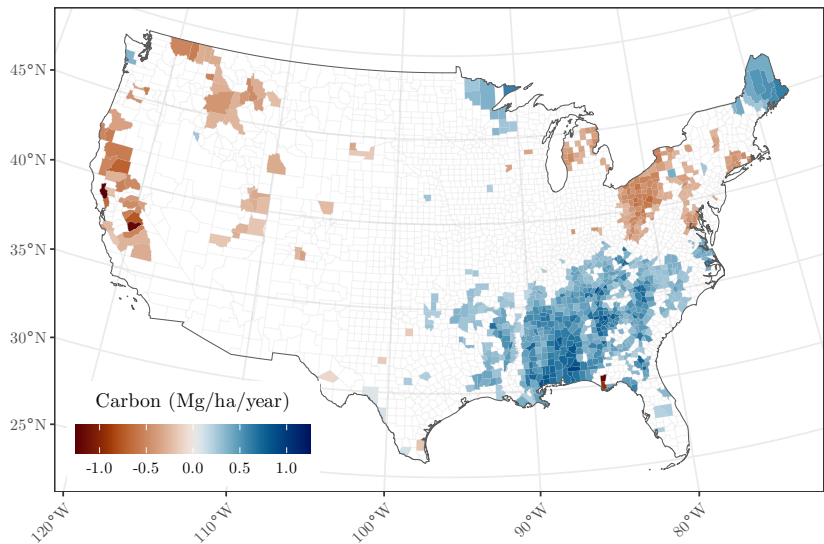


Washtenaw, Michigan



Estimator • Direct • Full model TCC —



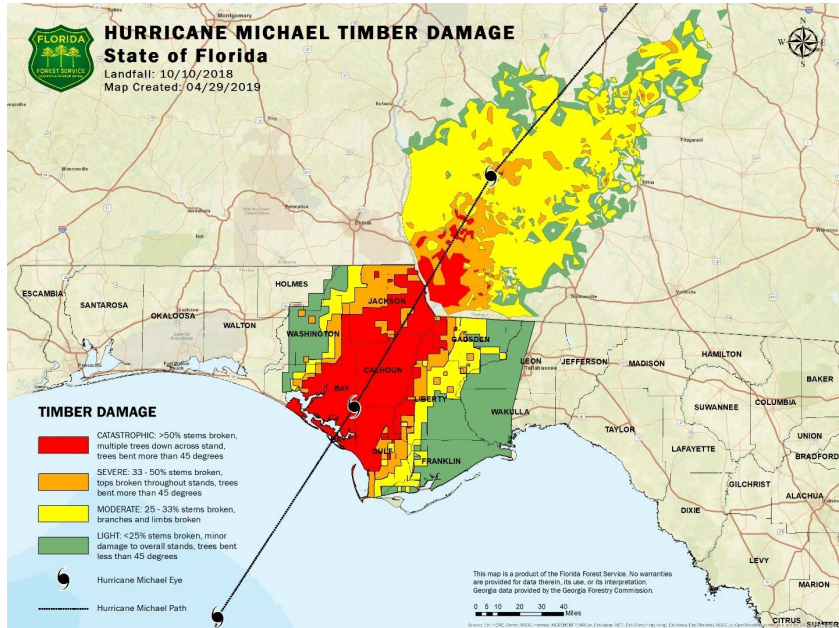




HURRICANE MICHAEL TIMBER DAMAGE

State of Florida

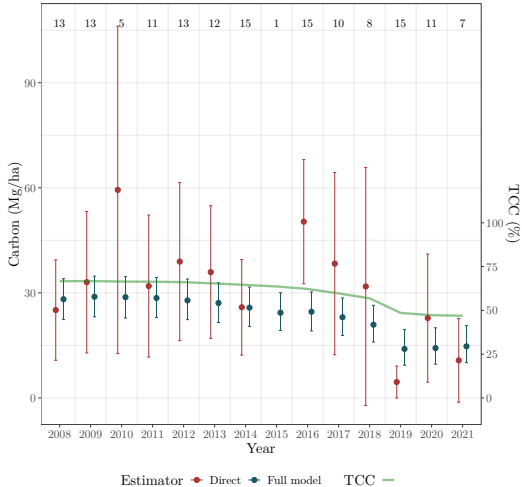
Landfall: 10/10/2018
Map Created: 04/29/2019



This map is a product of the Florida Forest Service. No warranties are provided for data therein, its use, or its interpretation. Georgia data provided by the Georgia Forestry Commission.

0 5 10 20 30 40

Calhoun, Florida



In 2018 the Hurricane Michael damaged much of the county's forestland.



Figure 4: Photo courtesy of Jarek Nowak, Ph.D., Florida Forest Service.

Next Steps

- Fit continue unit-level spatio-temporal SAE model.
- Fit dynamic unit-level spatio-temporal SAE model.
- Perform model comparison to explore if/how increasing information helps with FIA's desired annual county-level estimates.
- Extend models to multivariate settings for forest carbon pools.
- Explore patterns of changing carbon and work on attribution modeling.

Thank you

References I

- Banerjee, S., Carlin, B., and Gelfand, A. (2004). *Hierarchical Modeling and Analysis of Spatial Data*, volume 101.
- Coulston, J. W., Green, P. C., Radtke, P. J., Prisley, S. P., Brooks, E. B., Thomas, V. A., Wynne, R. H., and Burkhart, H. E. (2021). Enhancing the precision of broad-scale forestland removals estimates with small area estimation techniques. *Forestry: An International Journal of Forest Research*, 94(3):427–441.
- Datta, A., Banerjee, S., Finley, A. O., Hamm, N. A. S., and Schaap, M. (2016). Nonseparable dynamic nearest neighbor gaussian process models for large spatio-temporal data with an application to particulate matter analysis. *The Annals of Applied Statistics*, 10(3):1286–1316.
- Fay, R. E. and Herriot, R. A. (1979). Estimates of income for small places: An application of james-stein procedures to census data. *Journal of the American Statistical Association*, 74(366).

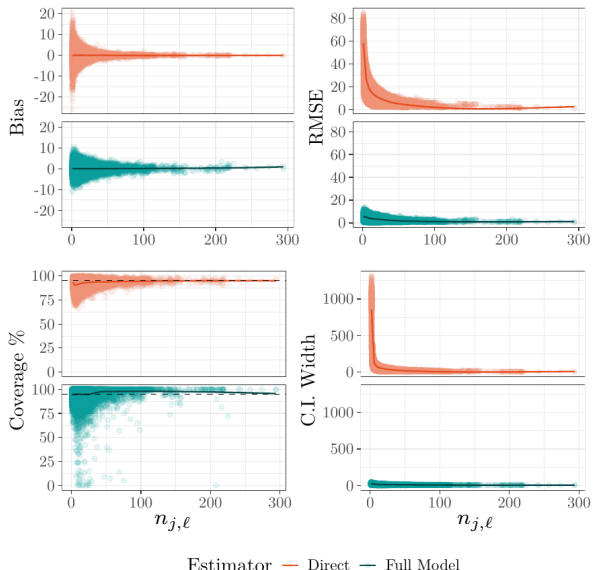
References II

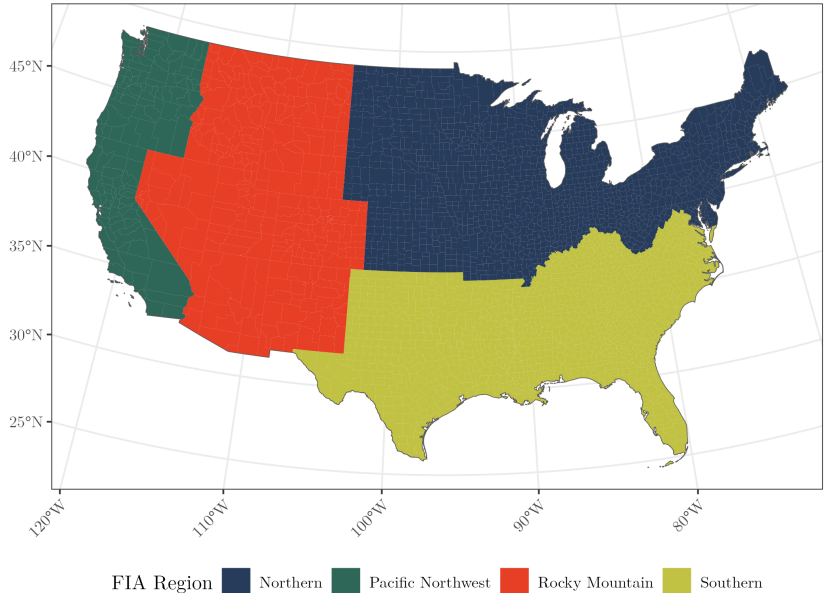
- Finley, A. O., Andersen, H.-E., Babcock, C., Cook, B. D., Morton, D. C., and Banerjee, S. (2024). Models to support forest inventory and small area estimation using sparsely sampled lidar: A case study involving g-liht lidar in tanana, alaska. *Journal of Agricultural, Biological and Environmental Statistics*.
- Hou, Z., Domke, G. M., Russell, M. B., Coulston, J. W., Nelson, M. D., Xu, Q., and McRoberts, R. E. (2021). Updating annual state-and county-level forest inventory estimates with data assimilation and FIA data. *Forest Ecology and Management*, 483:118777.
- Lister, A. J., Andersen, H., Frescino, T., Gatziolis, D., Healey, S., Heath, L. S., Liknes, G. C., McRoberts, R. E., Moisen, G. G., Nelson, M., et al. (2020). Use of Remote Sensing Data to Improve the Efficiency of National Forest Inventories: A Case Study from the United States National Forest Inventory. *Forests*, 11(12):1364.
- May, P. B. and Finley, A. O. (2025). Spatial-temporal models for forest inventory data.

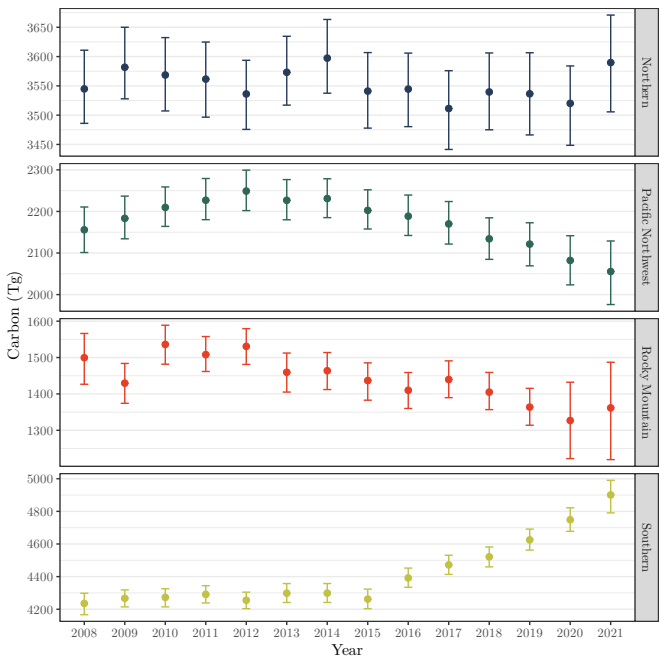
References III

- Schroeder, T. A., Healey, S. P., Moisen, G. G., Frescino, T. S., Cohen, W. B., Huang, C., Kennedy, R. E., and Yang, Z. (2014). Improving estimates of forest disturbance by combining observations from Landsat time series with US Forest Service Forest Inventory and Analysis data. *Remote Sensing of Environment*, 154:61–73.
- Shannon, E. S., Finley, A. O., Domke, G. M., May, P. B., Andersen, H.-E., Gaines III, G. C., and Banerjee, S. (2024). Toward spatio-temporal models to support national-scale forest carbon monitoring and reporting. *Environmental Research Letters*, 20(1):014052.
- Shannon, E. S., Finley, A. O., May, P. B., Domke, G. M., Andersen, H.-E., III, G. C. G., Nothdurft, A., and Banerjee, S. (2025). Leveraging national forest inventory data to estimate forest carbon density status and trends for small areas.

Simulation Study







Priors and Likelihood

The joint posterior distribution for all parameters in model (6) is then proportional to the product of the likelihood times priors, which is given as

$$\begin{aligned} & \prod_{\ell=1}^{\mathcal{L}} \prod_{j=1}^{\mathcal{J}} \prod_{i=1}^{n_{j,\ell}} N \left(y_{i,j,\ell} \mid \mathbf{x}_{j,\ell}^T \boldsymbol{\beta}_\ell + \tilde{\mathbf{x}}_{j,\ell}^T \boldsymbol{\eta}_j + u_{j,\ell}, \sigma_\ell^2 \right) \times \prod_{\ell=1}^{\mathcal{L}} IG \left(\sigma_\ell^2 \mid a_\sigma, b_\sigma \right) \times \\ & MVN \left(\boldsymbol{\beta}_0 \mid \boldsymbol{\mu}_0, \boldsymbol{\Sigma}_0 \right) \times \prod_{\ell=1}^{\mathcal{L}} MVN \left(\boldsymbol{\beta}_\ell \mid \boldsymbol{\beta}_{\ell-1}, \boldsymbol{\Sigma}_\xi \right) \times IW \left(\boldsymbol{\Sigma}_\xi \mid \nu_\xi, \mathbf{H}_\xi \right) \times \\ & \prod_{q=1}^Q MVN \left(\boldsymbol{\eta}_q^* \mid \mathbf{0}, \tau_{\eta,q}^2 \mathbf{Q}(\rho_{\eta,q}) \right) \times \prod_{q=1}^Q IG \left(\tau_{\eta,q}^2 \mid a_{\eta,q}, b_{\eta,q} \right) \times \prod_{q=1}^Q U \left(\rho_{\eta,q} \mid 0, 1 \right) \times \\ & \prod_{\ell=1}^{\mathcal{L}} MVN \left(\mathbf{u}_\ell \mid \mathbf{u}_{\ell-1}, \tau_{\omega,\ell}^2 \mathbf{Q}(\rho_\omega) \right) \times \prod_{\ell=1}^{\mathcal{L}} IG \left(\tau_{\omega,\ell}^2 \mid a_{\omega,\ell}, b_{\omega,\ell} \right) \times U \left(\rho_\omega \mid 0, 1 \right). \end{aligned} \tag{15}$$

Priors and Likelihood

The joint posterior distribution for all parameters in model (14) is then proportional to the product of the likelihood times priors, which is given as

$$\begin{aligned} & \prod_{j=1}^J \prod_{\ell=1}^{\mathcal{L}} N\left(\hat{\mu}_{j,\ell} \mid \mu_{j,\ell}, \sigma_{j,\ell}^2\right) \times \prod_{j=1}^J \prod_{\ell=1}^{\mathcal{L}} N\left(\mu_{j,\ell} \mid \mathbf{x}_{j,\ell}^T \boldsymbol{\beta} + \tilde{\mathbf{x}}_{j,\ell}^T \boldsymbol{\eta}_j + u_{j,\ell}, \sigma_{\epsilon}^2\right) \times \\ & MVN(\boldsymbol{\beta} \mid \boldsymbol{\mu}_{\beta}, \boldsymbol{\Sigma}_{\beta}) \times \prod_{j=1}^J \prod_{\ell=1}^{\mathcal{L}} IG\left(\sigma_{j,\ell}^2 \mid \frac{n_{j,\ell}}{2}, \frac{(n_{j,\ell}-1) \hat{\sigma}_{j,\ell}^2}{2}\right) \times \\ & IG\left(\sigma_{\epsilon}^2 \mid a_{\epsilon}, b_{\epsilon}\right) \times MVN\left(\mathbf{u} \mid \mathbf{0}, \sigma_u^2 \mathbf{R}(\rho_u) \otimes \mathbf{A}(\alpha_u)\right) \times \\ & IG\left(\sigma_u^2 \mid a_u, b_u\right) \times U(\rho_u \mid a_{\rho}, b_{\rho}) \times U(\alpha_u \mid a_{\alpha}, b_{\alpha}) \times \\ & \prod_{q=1}^Q MVN\left(\boldsymbol{\eta}_q^* \mid \mathbf{0}, \sigma_{\eta,q}^2 \mathbf{R}(\rho_{\eta,q})\right) \times \prod_{q=1}^Q IG\left(\sigma_{\eta,q}^2 \mid a_{\eta,q}, b_{\eta,q}\right) \times \prod_{q=1}^Q U(\rho_{\eta,q} \mid 0, 1). \end{aligned}$$